Estimation of V_{S30} by the HVSR Method at a Site in the Kathmandu Valley, Nepal

Rama M Pokhrel[1], Charlotte E L Gilder[2], Paul J Vardanega[3], Flavia De Luca[4], Maximilian J Werner[5] and Prem N Maskey[6]

Abstract

The SAFER (Seismic Safety and Resilience of Schools in Nepal) project work package "New generation seismic hazard for Nepal" aims to produce relevant outcomes for earthquake engineers working in Nepal. In order to improve disaster risk management, enhanced seismic hazard assessment is needed. Previous studies show there is insufficient geotechnical data in Kathmandu Valley to prepare a realistic hazard map. The SAFER project aims in part to collect and obtain new geotechnical data to assist with this aim. This paper presents data from a recent seismic microtremor test undertaken in the Kathmandu Valley.

Keywords: *HVSR; Kathmandu Valley;* V_{S30}

1. Introduction

The capital city of Nepal, Kathmandu was seriously damaged by the M_w 7.8 Gorkha earthquake in 2015 (Goda *et al.* 2015). The Kathmandu Valley is within a seismic prone region in Central Nepal and has been severely damaged in the past (e.g. Rana, 1935; Pandey & Molnar, 1988). The geotechnical and geophysical information available for seismic hazard assessment in Nepal is scarce (e.g. JICA, 2002). The SAFER (Seismic Safety and Resilience of Schools in Nepal) project commissioned two new boreholes in the Kathmandu Valley: for further details see Gilder *et al.* (2019). This paper presents results of a microtremor study at one of the SAFER borehole locations, in the Kathmandu Valley.

2. Geology of the Kathmandu Valley

As described by Sakai (2001) "The Kathmandu Basin is an intermontane basin located in the Central Himalaya and surrounded by mountains of 2,500 to 3,000 m above sea level". The basin originated by tectonic collision between the Indian and Eurasian plate, creating a complex thrust system which produced the Shivapuri mountain range to the north and Chandragiri and Phulchauki mountain ranges to the southwest and south respectively (Stöcklin, 1980). The geology of the Kathmandu Valley (for the purposes of seismic hazard assessment) can be considered to be in two main parts. First, are the metamorphic rocks (referred to as the 'basement') underlying the valley at depth, second is the overlying younger fluvio-deltaic, lacustrine and recent valley sediments. The distribution of these sediments is shown on the geological map presented in Fig. 1 which is based on the Department of Mines and Geology – Engineering and Environmental Geological Map of the Kathmandu Valley (Shrestha *et al.* 1998). At some localities the basement rocks within the valley floor protrude above the sediments.

The basement rocks are part of the Kathmandu Complex and form a synclinorium bounded by the Mahabharat Thrust (Stöcklin, 1980; Gehrels *et al.* 2006). Knowledge of the basement topography in

[1] Department of Civil Engineering, University of Bristol, Bristol, UK, r.pokhrel@bristol.ac.uk
[2] Department of Civil Engineering, University of Bristol, Bristol, UK, charlotte.gilder@bristol.ac.uk
[3] Department of Civil Engineering, University of Bristol, Bristol, UK, p.j.vardanega@bristol.ac.uk
[4] Department of Civil Engineering, University of Bristol, Bristol, UK flavia.deluca@bristol.ac.uk
[5] School of Earth Sciences, University of Bristol, Bristol, UK, max.werner@bristol.ac.uk
[6] Institute of Engineering, Tribhuvan University, Kathmandu, Nepal, pnmaskey@live.com

the Valley is important as it contributes to the unusual amplification effects seen within the Valley: a common phenomenon known to occur in basins (*Asimaki et al.* 2017). The depth of the basement has been estimated using gravity measurements to be at its deepest approximately 650 m beneath Baneswor (positioned centrally within the Valley) and reduces in thickness towards the Valley edges and outcropping bedrock (Moribayashi & Maruo, 1980). The thick semi-consolidated sediments are derived from the surrounding mountain ranges and are divided into seven main stratigraphic units (see Sakai et al. 2008 for overview of stratigraphic age relationships). The seven units categorised by Sakai et al. (2008) are the Dharmasthali, Kalimati, Gorkarna, Thimi, Tokha, and Patan Formations representing the northern part of the Valley, including again both the Patan and Kalimati, with additionally the Bagmati Formation for the central part of the Valley. Other stratigraphic units are described in the literature, including alternative ways of characterising the sediments such as Yoshida & Gautam (1988), and Sakai (2001), but perhaps represent an outdated perspective. Shrestha *et al.* (1998) present material units based on an engineering perspective, which remains a commonly used resource, as the distribution according to Shrestha *et al.* (1998) is presented on the engineering geology map (as in Fig. 1). However, the distribution of these sediments beneath the valley is uncertain as they consist of stratified and interfingering layers of sand, silts, clays and gravel with some carbonaceous mud, clay, and lithified organic matter (Sakai *et al.* 2008).

The Gokarna Formation is a fluvio-deltaic deposit only distributed in the northern part of the valley; around Gokarna, the Bishnumati river section, and north of Bhaktapur (Yoshida & Igarashi, 1984) comprising sand, silty clay and grey to dark brown peat (Yoshida & Igarashi, 1984). The Patan Formation is distributed mainly around Patan and Kathmandu city with isolated outcrops along Bagmati and Manohara rivers. This is considered to be a distal portion of the fluvio-deltaic depositional system, comprising laminated silt, clay, and peat layers with lesser amounts of sand. A deep borehole drilled for palaeo-climatic purposes reveals a sequence of black organic mud known as the Kalimati Clay which underlies the Valley at depth, outcropping centrally and within the southern portion of the Valley (Fujii & Sakai, 2002).

3. Geophysical Methods

3.1 Shear wave velocity in earthquake engineering

In design codes such as Eurocode 8 (CEN, 2004) the local soil conditions are classified by defining the average shear-wave velocity from the surface to 30m depth (V_{S30}). Shear-wave velocity can be measured using down-hole seismic, cross-hole seismic, and up-hole seismic methods (e.g., Luna & Jadi, 2000), Multichannel Analysis of Surface Wave (MASW) (e.g., Park *et al.* 1999); or microtremor measurement techniques (e.g., Tallett-Williams *et al.* 2016). Shear-wave velocity can also be estimated via correlations with parameters such as the Standard Penetration Test (SPT) *N* value (e.g., Ohta & Goto, 1978; Jafari *et al.* 2002; Dikmen, 2009; Gautam, 2017). Kriging analysis can mitigate the lack of data to some extent (e.g., Stein, 2012; Pokhrel *et al.* 2013). The major barrier to accurately preparing seismic hazard maps of the Kathmandu Valley is insufficient geotechnical data (e.g., Gilder *et al.* 2018). Analysis of the ground using non-invasive, passive techniques such as microtremor, is useful in the context of developing countries, where intrusive methods cannot be easily employed (Bard, 1999).

3.2 HVSR technique

The Horizontal to Vertical Spectral Ratio (HVSR) is a technique that can be used for the study of site response (Nakamura, 1989; Mucciarelli & Gallipoli, 2004; Mahajan *et al.* 2012; Flores *et al.* 2013). The HVSR technique records three components, two horizontal (perpendicular to each other) and one vertical, to measure the ambient seismic vibrations from the earth surface. Microtremors are made up of both natural and anthropogenic noise. The latter could be due to traffic, industrial vibrations etc. "The surface waves are assumed to be predominantly elliptical Rayleigh waves which are frequency dependant in a non-homogenous layered medium (Kramer 1996)" (Tallett-Williams *et al.* 2016). The main assumption associated with the method is that "a sharp peak (can be observed) at the fundamental frequency of the sediments, when there is a high impedance contrast between the sediments and underlying bedrock" (Gosar, 2017). While the method does have limitations, in a data scarce region, it provides quick assessment of the shear wave velocity at a specific location for use in seismic hazard assessment. The method has been used in the Kathmandu Valley in previous studies by Paudyal *et al.* (2012, 2013) and Tallett-Williams *et al.* (2016) who also used microtremor techniques in different locations in the Kathmandu Valley after the 2015 Gorkha earthquake.

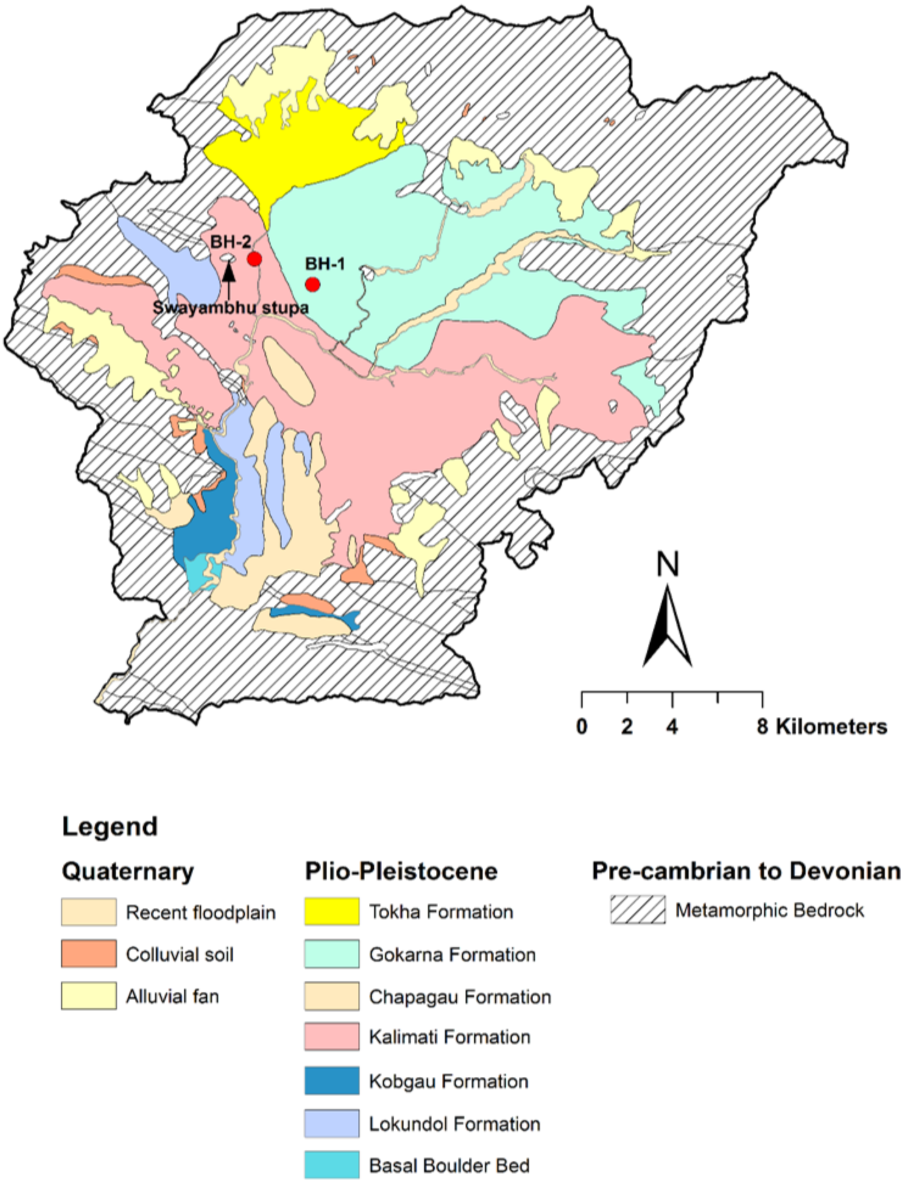

Fig. 1. Engineering and environmental geological map of Kathmandu Valley (modified from Shrestha *et al.* (1998) and location of SAFER boreholes BH-1 and BH-2.

4. Present Study

The SAFER project commissioned two boreholes (BH-1 and BH-2) and the locations are shown on Fig. 1 (Gilder *et al.* 2019). Analysis of the distribution of previously measured seismic shear wave velocity data assisted in the selection of the locations of the two SAFER boreholes, but also by identifying the optimal trade-off between geological and geotechnical interest of the area and vulnerability from earthquake hazard (e.g., vicinity to school buildings) (see Gilder *et al.* 2018 for further details). BH-1 is located in the school premises of the Padma Kanya School, Dillibazar [Fig. 2(a)] and BH-2 is located at Bijeshwori near Gita Mata School [Fig. 2(b)]. At BH-1, down-hole seismic testing was carried out and the results are reported in Gilder *et al.* (2019). The purpose of this paper is to present the results of the microtremor testing that was undertaken at the location of BH-2.

It was the intention of the authors to undertake downhole testing at both locations, however, during the period between boring and testing at BH-2 the borehole collapsed. The details of the borehole logs and geotechnical testing undertaken for both the boreholes are reported in a forthcoming paper (Gilder *et al.* 2019).

Fig. 2. Photos taken at (a) Kanya School Dillibazar (BH-1) and (b) Bijeshowri (BH-2) (Photos: R. M. Pokhrel)

4.1 Microtremor data and HVSR analysis

The field measurement of seismic ambient vibrations was undertaken using a Tromino® acquisition system. Fig. 3(a) shows the data collected with the system operating over a 20-minute period. Fig. 3(b) shows the azimuth of the recorded components.

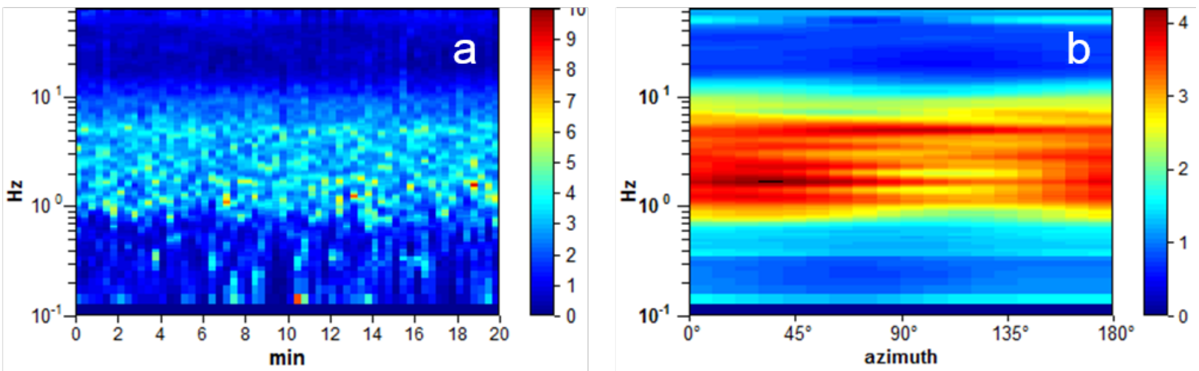

Fig. 3. Showing the time and directional history of the microtremor record (a) frequency-time history and (b) frequency-azimuth data. The colour scales indicate the relative amount of data acquired at each frequency interval (the images were taken as a screen shot during analysis by the software).

The analysis of the recording has been carried out in the software Grilla which accompanies the Tromino® portable instrument. This is undertaken by dividing the signal into windows of length (time in seconds). The Fast Fourier Transform (FFT) is then computed for each window (e.g., Kearey & Brooks, 1984). In this study a 20 second window was selected. Fig. 4(a) shows the three components, N-S, E-W and Up-Down. These spectra have been obtained using a triangular smoothing function with a width equal to 10%. The final average HVSR function is then computed within the software, obtained by averaging the HVSR at each window: shown as a red line in Fig. 4(b).

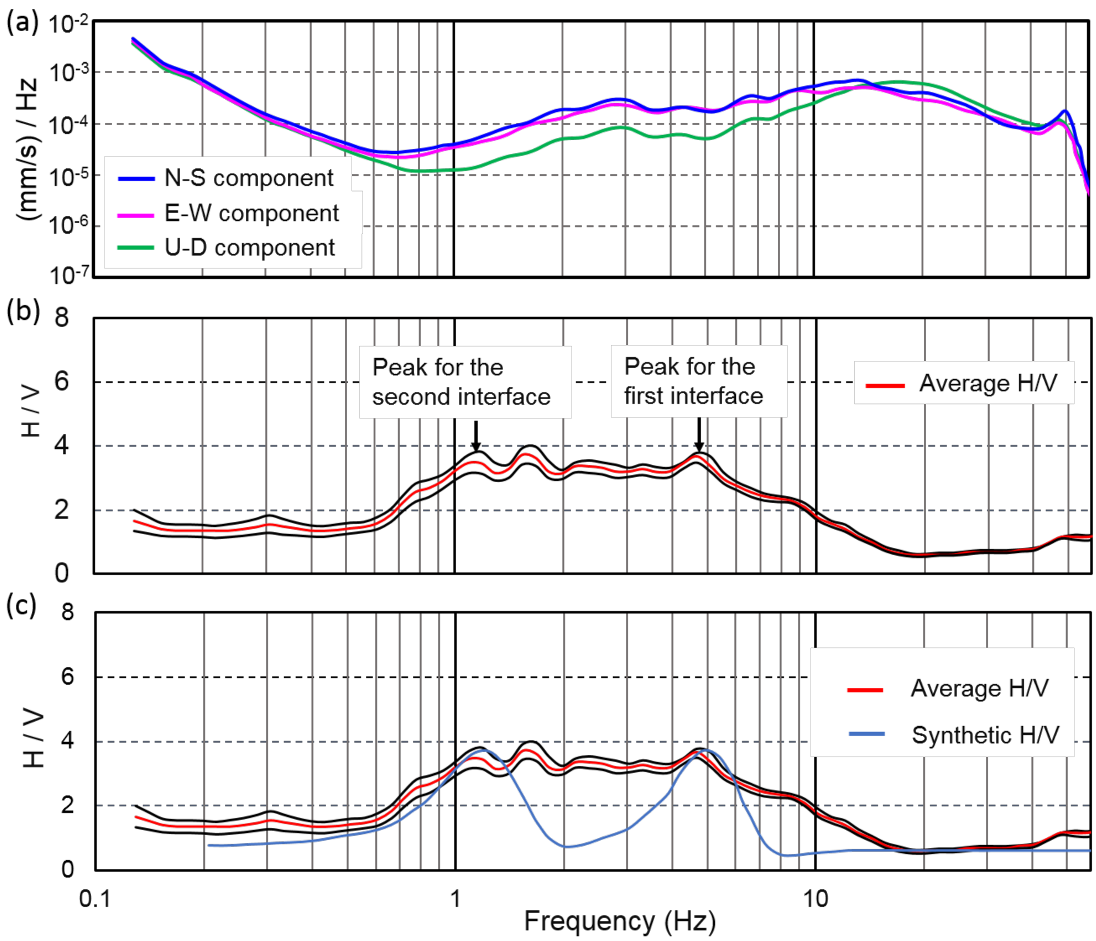

Fig. 4. (a) Converted recordings to the frequency domain using a Fast Fourier Transform (FFT), note the clear gap between horizontal and vertical components between 0.6 to 10 Hz. (b) H/V spectral ratios obtained at the site. The red line is the average H/V and black lines are the 95% confidence intervals. (c) Synthetic H/V spectra for Vs estimation from constrained H/V fitting (plots were digitised from output screenshots from the software).

In Fig. 4(a) there is a clear gap between the horizontal components (N-S and E-W lines) and the vertical component (U-D) from frequency 0.6 to 10, indicating the position in the spectra where frequencies are being amplified, due to a number of multi-reflections occurring at this interval (e.g., SESAME, 2004; Tallett-Williams *et al.* 2016). Fig. 4(b) shows the spectral ratio between horizontal and vertical ambient vibrations is shown in two clear peaks at points corresponding with overlap of N-S and E-W components of Fig. 4(a). The number of peaks depends on the number of stratigraphically contrasting layers. During the analysis the third peak seen in Fig. 4(b) did not meet the criteria of a clear H/V peak according to SESAME guidelines (SESAME, 2004). As the thickness of the surface layer is known from the borehole log to be about 11m, and the first peak is at a frequency of 5 Hz [depicted by the synthetic model shown in Fig. 4(c)] the velocity of the first layer is calculated by equation 1 (cf. Kramer 1996):

$$f_0 = Vs / (4T) \quad (1)$$

where f_0 is frequency, Vs is shear wave velocity and T is the thickness of each individual layer (cf. Kramer, 1996). The remaining shear wave velocities are then calculated using an iterative process within the software until a profile of site response is obtained. Although this method is not intended for use for identification of small-scale variation of shear wave velocity, the results from the microtremor technique can be used to indicate any large-scale velocity differences in the underlying sequence. The results indicate there are three layers with distinct shear wave velocities. This profile of shear wave velocity with predicted depth is presented in Fig. 5. Further details of this geophysical profile, including the depth, thickness, and velocities are presented in Table 1. It should be noted that the results presented in this paper are based on a single measurement i.e. an array pattern was not used.

The microtremor technique shows an upper layer exists from the ground surface to a depth of 11.5m below ground level (bgl), indicative of loose or soft soil with a predicted shear wave velocity of 220 m/s. Secondly, a middle layer of denser material with an estimated thickness of approximately 90m has a shear wave velocity of 470 m/s. Below 101.5 m depth the shear wave velocity is estimated to be approximately 900 m/s.

By way of comparison with design codes, V_{S30} values with velocities of above 800 m/s (CEN, 2004) or 760 m/s (ASCE, 2010) are attributed to be consistent with rock. Additionally, mean V_{S30} values of geological units in California indicate varying velocity with rock type, with sandstones, volcanic and metamorphic units ranging from 515 m/s to 782 m/s (see Table 1 in Wills & Clahan, 2006). The material types presented in Fig. 5 for Kathmandu are by geophysical interpretation. Similar past research (Paudyal *et al.* 2012 and 2013) show depths to velocities consistent with rock of approximately 96m bgl at the BH-2 location: this HSVR study indicates that velocities consistent with rock are present from 101.5m below ground level.

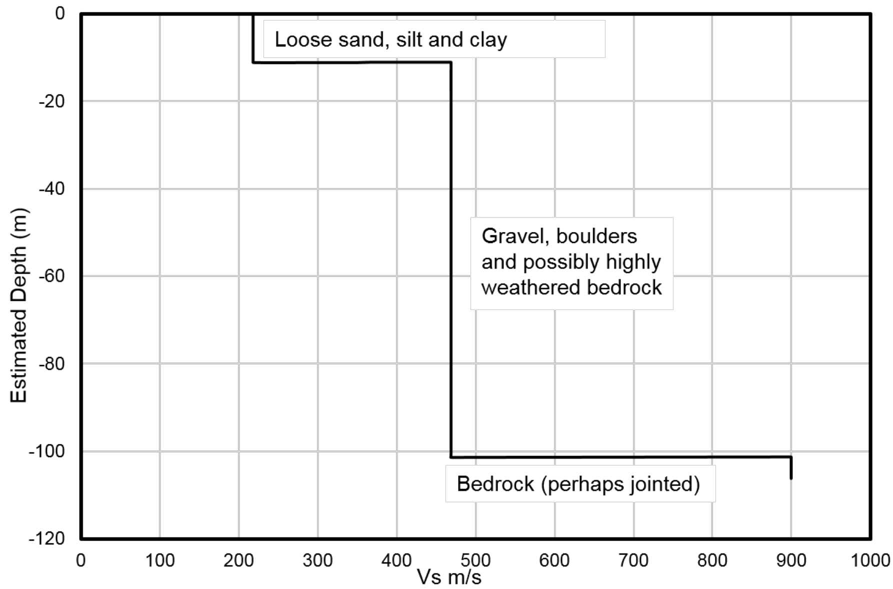

Fig. 5. The synthetically modelled Vs profile (data shown was digitised from the screenshots outputted by the analysis software)

Table 1: Results obtained from HVSR technique at BH-2

Depth at the bottom of the layer [m]	Thickness [m]	Vs [m/s]
1.5	11.5	220
101.5	90.0	470
Unproven (presumed bedrock)	not known	900

4.2 Comparison of microtremor data with the borehole records

For comparison with the microtremor data, the borehole log of the soil profile obtained at BH-2 is presented in Fig. 6. The log shows there below an initial layer of Made Ground there are soft (SPT-N values between 2 and 8) organic clayey silts extending from 1.90m to 10.85 m bgl. Below 10.85 m, a horizon of sandstone was encountered. This sandstone is shown in the photograph presented in Fig. 6(c). Interpretation of this layer is difficult due to the poor recovery and there is a lack of information regarding the fracture spacing and the orientation of these discontinuities. However, the layer can be assumed to be indicative of either an *in situ* highly weathered/fractured rock or alternatively a transported boulder of at least 9.25 m thick (proven to 20 m depth). In any case, the microtremor result indicates at this depth a layer of a lower shear wave velocity than would be expected for this type of deposit. An additional consideration is that the position of BH-2 is in an urban area of the valley, but also very near to the Swayambhu stupa, a hillock with bedrock exposure. Due to its location, just downhill of this outcrop, it is possible that the BH-2 site is at a marginal part of the valley, and the microtremor survey is underestimating the shear wave velocity at depth at this location.

Looking at the closest previous measurement of shear wave velocity at a location presented by JICA (2002), at the Fire Brigade Compound on New Road, in similar clayey silt materials of the Kalimati Formation, shear wave velocities of 118 m/s at 20 m depth and 220 m/s at 22 m depth were recorded. This is comparable to the values for the same materials presented in this study, even though the deposits are encountered at a shallower depth. The V_{S30} calculated for this location is 327 m/s.

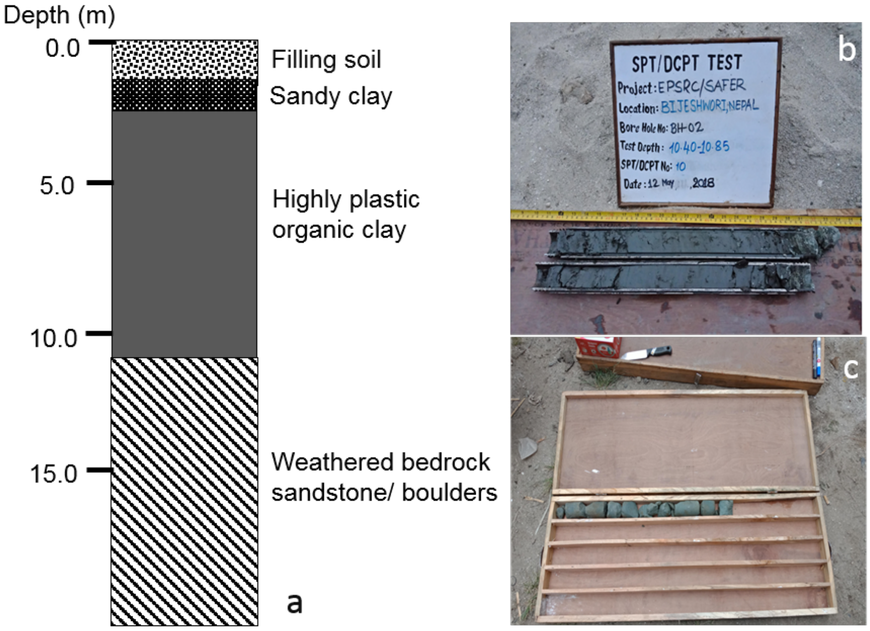

Fig. 6. (a) Record of the geotechnical borehole log at BH-2 (b) at the investigation site (BH-2) showing a photograph of a sample of the organic clay encountered between 1.70 m and 10.85 m in BH-2 (c) and core samples of bluish grey sandstone encountered between 10.85 m to 20.0 m depth (recovery representative of 9.15m of drilling) Photos: R. M. Pokhrel, 2018.

5. Conclusion

This paper presents the results of a microtremor investigation at the Bijeshwori site in the Kathmandu Valley. The microtremor data indicates that two intervals of high acoustic impedance exist: at around 11.0m and approximately 100 m below BH-2. At BH-2, the average shear wave velocity for the first 30m depth has been estimated at 327 m/s. The V_{S30} measured at this site is higher than the previously measured data available for the Kathmandu Valley. At this location it is suggested that the effect of the seismic response due to the site location on the edge of the basin is driving the amplification observed by the in the damage patterns exhibited in this part of the city and this may be outweighing the amplification effects due to soft sediments.

Further work is required to ascertain whether the sandstone encountered in BH-2 represents a boulder or fractured bedrock. If the subsurface is intact rock, presumably the value of V_{S30} would be even higher at this location if downhole shear wave measurements were taken. Given the uncertainties relating to the microtremor method, it is the view of the authors that the current depth to basement topography may currently be over-estimated using the microtremor technique, particularly in areas adjacent to the basement outcrops distributed throughout the valley.

Acknowledgements

The authors acknowledge the financial support from the Engineering and Physical Science Research Council (EPSRC) for the project "Seismic Safety and Resilience of Schools in Nepal" SAFER (EP/P028926/1). The second author acknowledges the support of EPSRC (EP/R51245X/1). Members of the consulting company Earth Investigation and Solution Nepal Pvt. Ltd, in particular, Surendra Shrestha, Dambar Shrestha, Raju Joshi are acknowledged for assisting with the drilling works and SPT testing carried out for the two new boreholes as part of the SAFER project. The authors thank geophysicist, Surendra Pant for performing the seismic survey. The digitised data used to reproduce Fig. 4 and 5 are available to bona fide researchers upon request.

References

American Society of Civil Engineers (2010). Minimum Design Loads for Buildings and Other Structures. ASCE/SEI 7-10, Reston, VA.

Asimaki, D., Mohammadi, K., Mason, H. B., Adams, R. K., Rajaure, S. and Khadka, D. (2017) Observations and Simulations of Basin Effects in the Kathmandu Valley During the 2015 Gorkha Earthquake sequence. *Earthquake Spectra*, 33(S1), S35 – S53.

Bard, P. V. (1999) Microtremor measurements: A tool for site effect estimation? In: The effects of Surface Geology on Seismic Motion, Irikura, Kudo, Okada and Sasatani (eds), Balkema, Rotterdam, The Netherlands, pp. 1251-1278.

CEN (European Committee for Standardization) (2004) Eurocode 8: Design of structures for earthquake resistance – Part 1: *General rules, seismic actions and rules for buildings*. Brussels, Belgium.

Dikmen, U. (2009) Statistical correlations of shear wave velocity and penetration resistance for soils. *Journal of Geophysics and Engineering*, 6(1), 61-72.

Flores, H., Malischewsky, P. and Jentzsch, G. (2013) H/V spectral ration analysis and Rayleigh modelization in eastern Thuringia, Germany. *Geofisica International*, 52(4), 355-364.

Fujii, R. and Sakai, H. (2002) Paleoclimatic changes during the last 2.5 myr recorded in the Kathmandu Basin, central Nepal Himalayas. *Journal of Asian Earth Sciences*, 20(3), 255-266.

Gautam, D. (2017) Empirical correlation between uncorrected standard penetration resistance (N) and shear wave velocity (Vs) for Kathmandu Valley, Nepal. *Geomatics, Natural Hazards and Risk*, 8(2), 496-508.

Gehrels, G.E., DeCelles, P.G., Ojha, T.P. (2006) Geologic and U-Th-Pb geochronologic evidence for early Paleozoic tectonism in the Kathmandu thrust sheet, central Nepal Himalaya. *Geological Society of America Bulletin,* 118(1-2), 185-198.

Gilder, C. E. L., Pokhrel, R. M., and Vardanega, P. J. (2019) A ground investigation to inform earthquake hazard assessment in the Kathmandu Valley, Nepal. *17th European Conference on Soil Mechanics and Geotechnical Engineering*, (XVII ECSMGE-2019), Reykjavik, Iceland, paper to be presented.

Gilder, C.E. L., De Risi, R., De Luca, F., Vardanega, P. J., Holcombe, E. A., Ayoubi, P., Asimaki, D., Pokhrel, R. M. and Sextos, A. (2018) Optimising resolution and improvement strategies for emerging geodatabases in developing countries. In: *Proceedings of the 16th European Conference on Earthquake Engineering*, European Association for Earthquake Engineering (EAEE), Paper No. 10743.

Goda, K., Kiyota, T., Pokhrel, R. M., Chiaro, G., Katagiri, T., Sharma, K. and Wilkinson, S. (2015) The 2015 Gorkha Nepal earthquake: insights from earthquake damage survey. *Frontiers in Built Environment,* 1, Article 8.

Gosar, A. (2017) Study on the applicability of the microtremor HVSR method to support seismic microzonation in the town of Idrija (W Slovenia). *Natural Hazards Earth System Science*, 17, 925-937.

Jafari, M. K., Shafiee, A. and Razmkhah, A. (2002) Dynamic properties of fine grained soils in south of Tehran. *Journal of Seismology and Earthquake Engineering*, 4(1), 25-35.

JICA (Japan International Co-operation Agency) (2002) The study on Earthquake Disaster Mitigation in the Kathmandu Valley, Kingdom of Nepal. Final Report, Volume I-IV.

Kearey, P., and Brooks, M. (1984) An Introduction to Geophysical Exploration (Second Addition). Blackwell Scientific Publications, London, United Kingdom.

Kramer S. L. (1996) *Geotechnical Earthquake Engineering*. Prentice Hall, New York, USA.

Luna, R. and Jadi, H. (2000) Determination of Dynamic Soil Properties Using Geophysical Methods. In: *Proceedings of the first International Conference on the Application of Geophysical and NDT methodologies to Transportation Facilities and Infrastructure*, St. Louis, MO.

Mahajan, A. K., Mundepi, A. K., Chauhan, N., Jasrotia, A. S., Rai, N. and Gachhayat, T. K. (2012) Active seismic and passive microtremor HVSR for assessing site effects in jammu city, NW Himalaya, India-A case study. *Journal of Applied Geophysics,* 77, 51-62.

Moribayashi, S. and Maruo, Y. (1980) Basement topography of the Kathmandu Valley, Nepal- an application of gravitational method to the survey of a tectonic basin in the Himalayas. *Journal of Japan Society of Engineering Geology*, 21(2), 30-37.

Mucciarelli, M. and Gallipoli, M. R. (2004) The HVSR technique from microtremor to strong motion: empirical and statistical considerations. In: *Proceeding of 13th World conference on Earthquake Engineering*, Vancouver, B. C., August 1-6, 2004, Paper no. 45.

Nakamura, Y. (1989) Method for dynamic characteristics estimation of subsurface using microtremor on the ground surface. *Railway Technical Research Institute, Quarterly Reports*, 30(1), 25-33.

Ohta, Y. and Goto, N. (1978) Empirical shear wave velocity equations in terms of characteristic soil indexes. *Earthquake Engineering and Structural Dynamics*, 6(2), 167-187.

Pandey, M. R., and Molnar P. (1988) The distribution of intensity of the Bihar–Nepal earthquake 15 January 1934 and bounds of the extent of the rupture zone. *Journal of Nepal Geological Society*, 5, 22-44.

Park, C. B., Miller, R. D. and Xia, J. (1999) Multichannel analysis of surface waves. *Geophysics*, 64(3): 800-808.

Paudyal, Y. R., Yatabe, R., Bhandary N. P. and Dahal, R. K. (2012) A study of local amplification effect of soil layers on ground motion in the Kathmandu Valley Using microtremor analysis. *Earthquake Engineering and Engineering Vibration*, 11(2), 257-268.

Paudyal, Y. R., Yatabe, R., Bhandary, N. P. and Dahal, R. K. (2013). Basement topography of the Kathmandu Basin using microtremor observation. *Journal of Asian Earth Sciences*, 62, 627-637.

Piya, B. K. (2004) Generation of a Geological database for the liquefaction hazard assessment in Kathmandu valley. *MSc thesis*, International Institute for Geo-information Science and Earth Observation, Enschede, The Netherlands.

Pokhrel, R. M., Kuwano, J. and Tachibana, S. (2013) A kriging method of interpolation used to map liquefaction potential over alluvial ground. *Engineering Geology*, 152(1), 26-37.

Rana, B. S. (1935) *Nepal Ko Maha Bhukampa (The great earthquake of Nepal)*. Jorganesh Press, Kathmandu (in Nepali).

Sakai, H. (2001) The Kathmandu Basin: an archive of Himalayan uplift and past monsoon climate. *Journal of Nepal Geological Society,* 25(Special Issue), 1-8

Sakai, T., Gajurel, A. P., Tabata, H., Ooi, N., Takagawa, T., Kitagawa, H., and Upreti, B. N. (2008) Revised lithostratigraphy of fluvio-lacustrine sediments comprising northern Kathmandu basin in central Nepal. *Journal of Nepal Geological Society*, 37, 25-44.

SESAME (Site EffectS assessment using AMbient Excitations) (2004) Guidelines for the implementation of the H/V spectral ratio technique on ambient vibrations: measurements, processing and interpretation. SESAME European Research Project WP12, deliverable D23.12. Available from: < http://sesame.geopsy.org/Papers/HV_User_Guidelines.pdf > (accessed 17/02/2019).

Shrestha, O. M., Koirala, A., Karmacharya, S. L., Pradhananga, U.B., Pradhan, R., and Karmacharya, R. (1998) Engineering and environmental geological map of the Kathmandu Valley (1:50,000) Dept. Mines and Geology, His Majesty's Government of Nepal.

Stein, M. L. (2012) *Interpolation of spatial data: some theory for kriging*. Springer Science & Business Media.

Stöcklin, J. (1980) Geology of Nepal and its regional Frame. *Journal of the Geological Society of London*, 137, 1-34.

Tallett-Williams, S., Ghosh, B., Wilkinson, S., Fenton, C. Burton, P., Whitworth, M., Datla, S., Franco, G., Trieu, A., Dejong, M., Novellis, V, White, T. and Lloyd, T. (2016) Site amplification in the Kathmandu Valley during the 2015 M7.6 Gorkha, Nepal earthquake. *Bulletin of Earthquake Engineering*, 14(12), 3301-3315.

Wills, C. J. and K. B. Clahan (2006). Developing a map of geologically defined site-condition categories for California, *Bulletin of the Seismological Society of America,* 96(4A), 1483–1501.

Yoshida, M. and Gautam, P. (1988) Magnetostratigraphy of Plio-Pleistocene Lacustrine Deposits in the Kathmandu Valley, Central Nepal. *Proceedings of the National Academy of Sciences, India*, 54, A, 3: 410-417.

Yoshida, M. and Igarashi, Y. (1984) Neogene to Quaternary Lacustrine Sediments in the Kathmandu Valley, Nepal. *Journal of Nepal Geological Society*, 4(Special Issue), 73-100.